

**POLLUCITE AND THE CESIUM-DOMINANT ANALOGUE  
OF POLYLITHIONITE AS EXPRESSIONS OF EXTREME Cs ENRICHMENT  
IN THE YICHUN TOPAZ–LEPIDOLITE GRANITE, SOUTHERN CHINA**

RU CHENG WANG, HUAN HU AND AI CHENG ZHANG

*State Key Laboratory for Mineral Deposits Research, Department of Earth Sciences,  
Nanjing University, Nanjing 210093, People's Republic of China*

XIAO LONG HUANG

*Guangzhou Institute of Geochemistry, Chinese Academy of Sciences, Guangzhou, Wushan 510640,  
People's Republic of China*

PEI NI

*State Key Laboratory for Mineral Deposits Research, Department of Earth Sciences,  
Nanjing University, Nanjing 210093, People's Republic of China*

ABSTRACT

The Yichun topaz–lepidolite granite is the youngest and most evolved unit of the Yichun granitic complex, southern China, and is well known by virtue of the unusual development of Ta–Nb–Li mineralization and enrichment in cesium in a granite. Three petrographic zones are recognized from the bottom upward: K-feldspar-rich facies, albite-rich facies, and albite- and K-feldspar-rich facies. The Cs contents increase with fractional crystallization of the magma, and reach a maximum in the middle part of the albite-rich facies (1709 ppm). Two principal carriers of Cs are observed in this facies: pollucite and the Cs-dominant analogue of polyolithionite. In the middle part of this facies, both minerals occur as small inclusions within quartz or K-feldspar phenocrysts, indicative of a magmatic origin. However, in the upper part of this facies, pollucite appears interstitially among tabular crystals of albite around K-feldspar phenocrysts, suggesting that this type of pollucite postdates the rock-forming minerals, but formed prior to complete crystallization of the silicate melt. In addition, Cs-rich replacement zones typify the rim of lepidolite flakes in the groundmass. Lepidolite may contain up to 25.8 wt% Cs<sub>2</sub>O, or ~0.9 Cs *apfu* (based on O = 11). Such lepidolite may be considered a Cs-dominant analogue of polyolithionite. According to their distribution and compositional characteristics, pollucite and the Cs-dominant analogue of polyolithionite seem to have formed at the late-magmatic or magmatic to hydrothermal transition stage of evolution of the leucogranitic magma at Yichun.

*Keywords:* pollucite, Cs-dominant analogue of polyolithionite, cesium, electron-microprobe data, granite, Yichun, China.

SOMMAIRE

Le granite à topaze–lépidolite de Yichun, l'unité la plus tardive et la plus évoluée du complexe granitique de Yichun, du Sud de la Chine, est bien connu à cause de sa minéralisation inhabituelle en Ta–Nb–Li, et son enrichissement en Cs. Trois zones pétrographiques ont été subdivisées du bas en haut: faciès riche en feldspath potassique, faciès albitique et faciès enrichi en deux feldspaths. La concentration de Cs augmente avec la cristallisation du magma, jusqu'à 1709 ppm au milieu du faciès albitique. En conséquence, deux types de porteurs de Cs sont observés: la pollucite et l'analogue à dominance de Cs de la polyolithionite. Au milieu du faciès, elles sont présentes sous forme de petites inclusions dans les phénocristaux de quartz et feldspath potassique, indiquant une origine magmatique. Cependant, vers le haut du faciès, la pollucite remplit les espaces parmi les cristaux tabulaires d'albite; ce type de pollucite serait donc postérieur aux minéraux majeurs, mais il s'est formé avant la cristallisation complète du liquide silicaté. De plus, des zones de remplacement riches en Cs caractérisent la bordure de paillettes de lépidolite. La lépidolite peut contenir jusqu'à 25.8 % de Cs<sub>2</sub>O (poids), ou environ 0.9 atomes de Cs par unité formulaire (sur la base de 11 O). Telle lépidolite peut être considérée comme un analogue à Cs dominant de la polyolithionite. D'après leur distribution et caractéristiques

§ *E-mail address:* rcwang@nju.edu.cn

chimiques, les porteurs de Cs semblent cristalliser à un stade magmatique tardif ou à la transition magmatique à hydrothermale au cours de l'évolution du magma leucogranitique à Yichun.

*Mots-clés:* pollucite, analogue à Cs dominant de la polyolithionite, césium, données de microsonde électronique, granite, Yichun, Chine.

## INTRODUCTION

Cesium occurs generally diluted in traces in potassium-bearing minerals, owing to its very low clarke value (2 ppm, McDonough *et al.* 1992) and large ionic radius (1.67 Å, Shannon 1976). Pollucite is the most important mineral of cesium, commonly found in evolved pegmatite rocks. Furthermore, nanpingite, the Cs analogue of muscovite, was first described in the Nanping rare-element granitic pegmatite in southern China (Yang *et al.* 1988, Ni & Hughes 1996). Simmons *et al.* (2001) have recently described the new species *londonite* from the Antandrokomby granitic pegmatite, in Madagascar; it is the Cs-dominant analogue of rhodizite. It is obvious that these Cs minerals occur in pegmatitic rocks owing to protracted fractionation, as was documented, *e.g.*, in Tanco, Manitoba, Canada (Teertstra *et al.* 1992), Bikita, Zimbabwe (Teertstra & Černý 1997) or Altai, northwestern China (Wang *et al.*, in prep.). Although rarely documented in the literature to date, an enrichment in Cs is also possible in highly fractionated granites, as demonstrated in the Beauvoir rare-element granites, Massif Central, France (whole-rock Cs content up to 664 ppm: Rossi *et al.* 1987), as well as in the Yichun topaz–lepidolite granite, southern China (whole-rock Cs content up to 1709 ppm: Huang *et al.* 2002). Very recently, on the basis of a melt-inclusion study of two granites in northern New Mexico, Audétat & Pettke (2003) have shown that during progressive crystallization and fluid exsolution, the Cs contents of the residual melt increased from 1 ppm to values as high as 5500 ppm. Furthermore, an inclusion of pollucite in albite was reported in the B2 facies of the Beauvoir topaz granite (Rossi *et al.* 1987). During previous work in the Yichun topaz–lepidolite granite, investigations have also demonstrated the common presence of both pollucite and Cs-enriched, even Cs-dominant, lepidolite-series minerals. Our paper deals with a detailed presentation of the mineralogical features of Cs-bearing minerals from the Yichun topaz–lepidolite granite, and a discussion of enrichment processes of cesium at the magmatic to hydrothermal stage of evolution of the granite.

## GEOLOGICAL SETTING OF THE YICHUN GRANITE

The characteristics of the Yichun topaz–lepidolite granite have been discussed in an earlier publication (Huang *et al.* 2002). We give here a simplified geological map of the granite pluton with a cross-section, and the location of samples taken in a 43-m-deep drillhole

and quarries in the section (Fig. 1). Five units can be recognized in the Yichun granite pluton, but the topaz–lepidolite granite is the only one to be mineralized (Ta, Nb, Sn, Li). The topaz–lepidolite granite itself can be subdivided into three facies from the bottom upward: (1) a K-feldspar-rich facies, (2) an albite-rich facies, and (3) an albite- and K-feldspar-rich facies (Fig. 1, Huang *et al.* 2002). This granite is highly evolved, with economic concentrations of disseminated rare metals such as Ta, Nb, Zr, Hf and Be. It shows enrichment in rare alkalis such as Li, Rb and Cs. In particular, Cs contents increase with progressive crystallization of the granite, and reach the highest level in the middle part of the albite-rich facies (*e.g.*, Zk05: 1709 ppm, Fig. 1). Two principal minerals containing the cesium (pollucite and Cs-rich lepidolite-series mineral) have been found in this granite, and their compositions are very sensitive monitors of the physicochemical conditions of their environment of crystallization in the leucogranitic magma.

## ANALYTICAL METHODS

Polished thin sections were initially examined using the back-scattered electron (BSE) mode of a JEOL JXA8800 electron microprobe in the Department of Earth Sciences, Nanjing University, in order to characterize the internal chemical heterogeneity of the Cs minerals. Mineral compositions were determined with the same electron microprobe, equipped with three wavelength-dispersion spectrometers. The operating conditions were as follows: accelerated voltage 15 kV, beam current 20 nA, beam diameter 1 µm. Both natural and synthetic standards were used: Amelia albite (Na), Tanco pollucite (Cs, Al, Si), orthoclase (K), amazonitic K-feldspar (Rb), hornblende (Mg, Fe, Ca), Durango fluorapatite (F). We used the ZAF program for data reduction (Armstrong 1989). The lithium content of lepidolite was estimated according to the empirical equation proposed by Tindle & Webb (1990):  $\text{Li}_2\text{O (wt\%)} = (0.287 \times \text{SiO}_2) - 9.552$ .

In order to identify the Cs-rich lepidolite-series mineral, Raman spectra were recorded at room temperature on polished thin sections with a Renishaw RM2000 micro-Raman spectrometer equipped with a CCD detector, also in the Department of Earth Sciences of Nanjing University. The operating conditions were as follows: excitation laser wavelength: 514 nm (Ar<sup>+</sup> laser), laser energy: 5 mW, and spectral slit: 25 µm. The 50× objective was used on a Leica DM/LM microscope. With this objective, the lateral spot-size of the

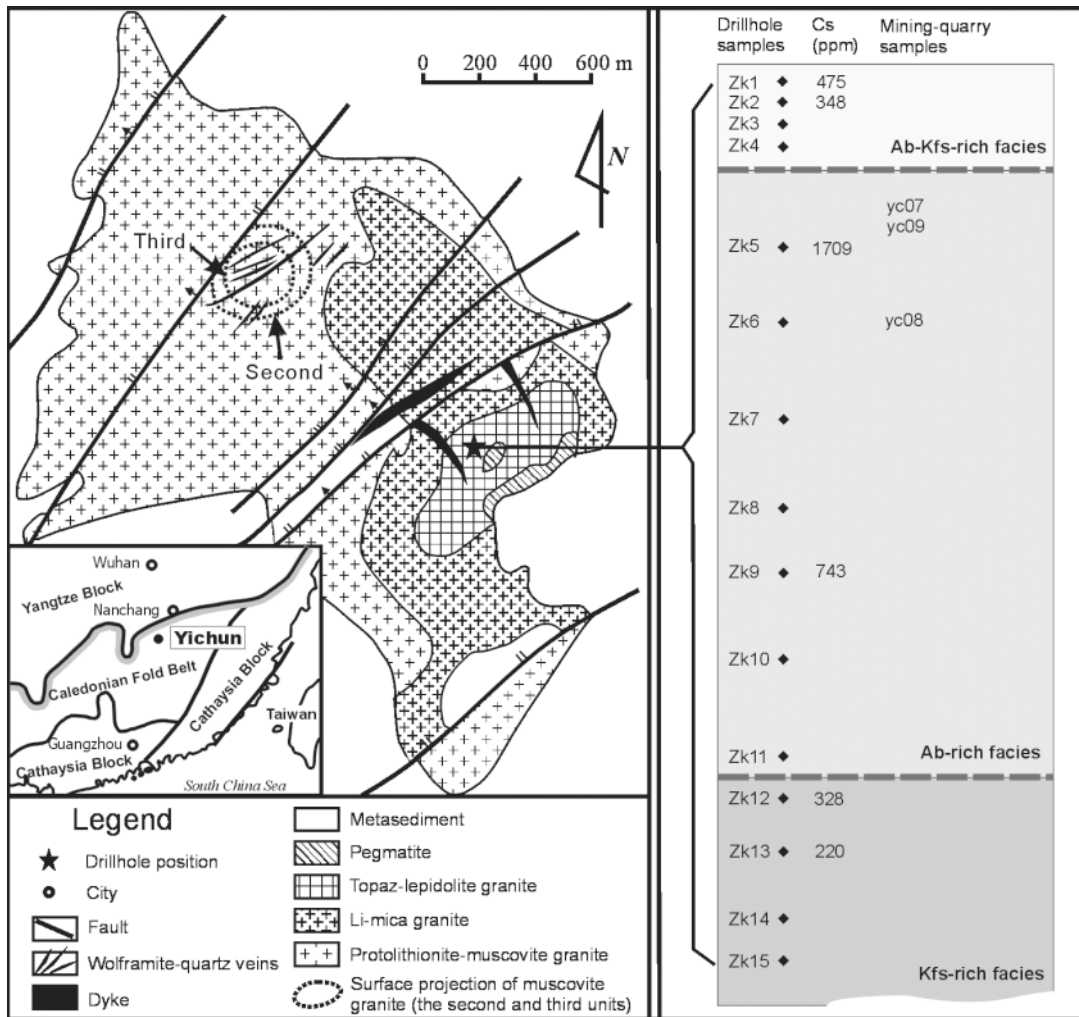


FIG. 1. Geological map (after Yin *et al.* 1995) and simplified cross-section of the Yichun topaz-lepidolite granite. Whole-rock Cs contents of selected drill-hole samples are also given.

laser beam was about 1  $\mu\text{m}$ . Silicon ( $520\text{ cm}^{-1}$  Raman shift) was used as a standard. The Raman spectrum was collected in 30 minutes.

#### THE COMPOSITION OF THE POLLUCITE

Pollucite, ideally  $\text{CsAlSi}_2\text{O}_6$ , is a member of the leucite – analcime family of cubic and pseudocubic zeolite-related minerals. The cations Cs, Rb, and K substitute for each other in one site in the pollucite structure (grouped as the CRK component; defined as  $100(\text{Cs} + \text{Rb} + \text{K}) / \sum(\text{Na} + \text{K} + \text{Rb} + \text{Cs} + \text{Mg} + \text{Ca})$  Beger 1969, Černý 1974), which also contains molecular  $\text{H}_2\text{O}$ .

The solid solution of analcime toward pollucite generally entails substitution of  $\text{H}_2\text{O}$  in analcime for a CRK cation, accompanied by the introduction of charge-balancing Na on a second site (Teertstra *et al.* 1992). The general formula for pollucite – analcime solid solutions is stated to be  $(\text{Cs}_x\text{Na}_y)\text{Al}_{1+x-y}\text{Si}_{3-x-y}\text{O}_6 \cdot (1-x)\text{H}_2\text{O}$  ( $2y < 1-x < y$ , and  $x \approx 0.90$ ), which indicates that Si/Al exceeds 2 across the series.

In the Yichun granite body, pollucite was observed in two different modes of occurrence. It is found as inclusions in quartz, and as interstitial crystals among albite.

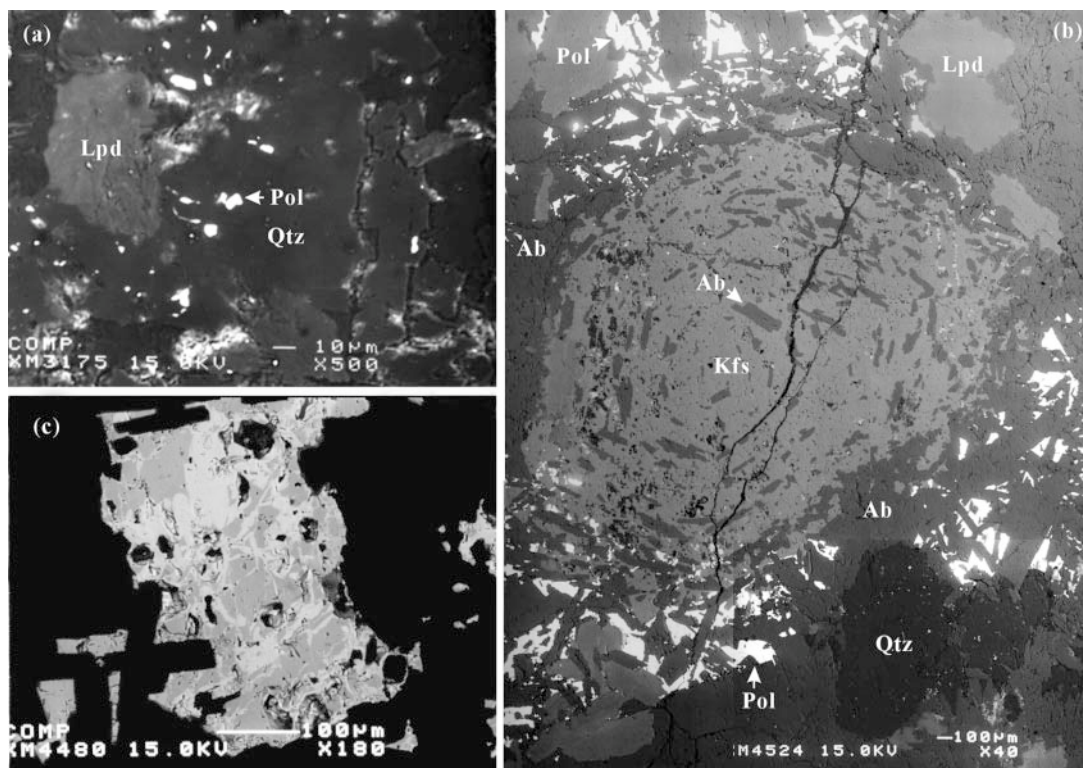


Fig. 2. Back-scattered electron images of pollucite. (a) Micro-inclusions of pollucite enclosed in quartz (bright dots). (b) Pollucite fillings of interspaces of albite crystals around a K-feldspar phenocryst. (c) Heterogeneous crystal of pollucite. Symbols: Qtz (quartz), Kfs (K-feldspar), Ab (albite), Lpd (lepidolite), Pol (pollucite).

#### *Pollucite inclusions in quartz*

In the middle part of the albite-rich facies (ZK5, 6, 7, YC08), pollucite is found as inclusions within quartz (Fig. 2a). Such mineral paragenesis indicates that pollucite predates the crystallization of the rock-forming minerals, and is further likely to be of near-liquidus magmatic origin. The pollucite grains are very fine, generally micrometric, with variable forms, but more commonly oval or rounded.

Electron-microprobe results show that the compositions of pollucite range from 32.2 to 36.6 wt%  $\text{Cs}_2\text{O}$  (Table 1). In a plot of Si/Al versus CRK, Si/Al ranges from 2.24 to 2.54, and CRK, from 77.02 to 86.22 (Fig. 3). Pollucite from the Yichun granite has an almost identical composition to pollucite from other worldwide localities (Fig. 3).

#### *Interstitial pollucite between albite crystals*

In the Yichun topaz-lepidolite granite, the “snowball”-textured K-feldspar phenocrysts are characteristic. The “snowball” texture is named specially for the K-

feldspar phenocrysts containing fine tabular crystals of albite along their growth zones in rare-element granites (Yin *et al.* 1995). The  $\text{P}_2\text{O}_5$  contents in the host K-feldspar and albite inclusions have already been investigated (Huang *et al.* 2002). In this study, we found further that the K-feldspar phenocrysts contain small patches of Cs-rich lepidolite in the middle facies, ZK05, 06 and 07 (see below for details). However, in the upper part of the albite-rich facies (yc09), phenocrysts of K-feldspar are free of Cs-rich lepidolite. In contrast, pollucite was found at their rims and as intergranular fillings between tabular crystals of albite (Fig. 2b), which surround the K-feldspar phenocryst. This type of pollucite thus post-dates the main rock-forming minerals (*e.g.*, K-feldspar or albite). The pollucite crystals are up to a few hundreds micrometers in size.

Back-scattered-electron images show that the pollucite is heterogeneous, characterized by two parts of distinct brightness. It is mainly darker, but some lighter parts penetrate (Fig. 2c); the former is the primary phase, whereas the latter represents an altered product. Accordingly, electron-microprobe data reveal obvious compositional differences between them. The

primary pollucite has Si/Al from 2.20 to 2.43, CRK from 69.56 to 75.61 (Table 1, Fig. 3). In comparison, the altered phase is richer in Cs and Al, as revealed by its higher CRK (75.42 to 81.51) and lower Si/Al ratio (2.15 to 2.33) (Table 1, Fig. 3).

#### THE COMPOSITION OF THE CS-BEARING LEPIDOLITE-SERIES MINERAL

Known examples of Cs-bearing mica to date include nanpingite ( $\text{Cs}_2\text{O} = 25.29$  wt%, Yang *et al.* 1988), cesian biotite ( $\text{Cs}_2\text{O} = 5.97$  wt%, Ginsburg *et al.* 1972) and rubidian cesian phlogopite ( $\text{Cs}_2\text{O} = 6.60$  wt%, Hawthorne *et al.* 1999). Nanpingite, ideally  $\text{CsAl}_2\text{AlSi}_3\text{O}_{10}(\text{OH})_2$ , is the Cs analogue of muscovite. Ercit *et al.* (2003) mentioned existence of Cs-rich lepidolite in association with pollucite as a pocket phases in a lithium pegmatite of the O'Grady batholith, in the Northwest Territories, Canada, though no electron-microprobe data were obtained. Very recently, Černý *et al.* (2003) described the mode of occurrence and chemical composition of five types of micas with Rb- or Cs-dominant populations from the Red Cross Lake rare-element pegmatites in north-central Manitoba. The lepidolite from the Yichun

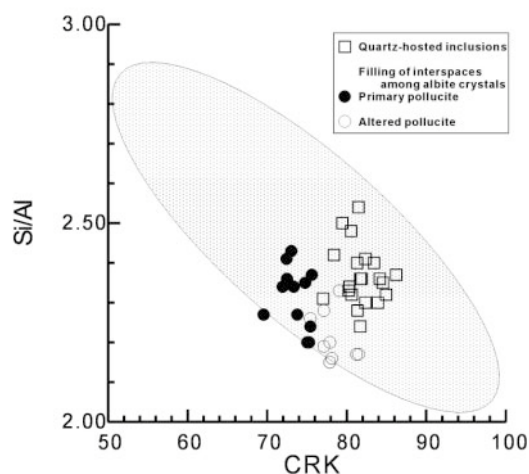


FIG. 3. Compositional trends of pollucite in the Si/Al versus CRK diagram. Shaded ellipse: range of pollucite from pegmatites, drawn using data of Černý & Simpson (1978), Teertstra *et al.* (1992) and Teertstra & Černý (1995, 1997).

TABLE 1. REPRESENTATIVE COMPOSITIONS OF POLLUCITE FROM THE YICHUN TOPAZ–LEPIDOLITE GRANITE, SOUTHERN CHINA

	Inclusions in quartz						Fillings of interstices among albite crystals					
	Zk-5		Zk-6		Zk-7		Yc09					
	1	2	3	13	7	11	1	4	11	10	13	12
							(D)	(B)	(D)	(B)	(D)	(B)
SiO <sub>2</sub> wt%	45.62	45.24	45.31	44.79	43.77	44.70	48.83	43.54	47.75	43.46	48.61	43.62
Al <sub>2</sub> O <sub>3</sub>	16.67	16.50	16.01	16.23	16.00	15.98	18.24	17.12	17.33	16.99	17.43	17.03
FeO	0.02	–	–	–	0.04	–	0.01	0.05	0.05	–	0.05	0.11
MnO	–	0.03	–	–	–	–	0.03	–	–	0.02	0.01	–
MgO	0.03	–	–	–	–	0.01	0.04	–	–	0.04	–	–
Na <sub>2</sub> O	1.69	1.85	1.48	1.87	1.43	1.27	2.70	2.15	2.68	1.76	2.16	1.86
K <sub>2</sub> O	0.10	0.06	0.03	0.01	0.01	0.05	0.02	0.00	0.02	0.02	0.02	0.00
Rb <sub>2</sub> O	0.08	0.12	0.07	–	0.06	0.12	–	0.04	0.05	–	0.04	0.07
Cs <sub>2</sub> O	32.24	33.83	33.71	34.75	36.63	36.23	28.69	34.92	31.16	35.80	30.44	36.50
CaO	0.02	0.01	0.01	0.01	–	0.01	0.05	0.01	–	–	0.01	–
P <sub>2</sub> O <sub>5</sub>	0.03	0.01	0.02	–	–	0.01	0.46	–	0.47	–	0.46	–
Total	96.50	97.65	96.64	97.68	97.94	98.38	99.07	97.83	99.51	98.09	99.23	99.18
Si <i>apfu</i>	2.114	2.108	2.130	2.108	2.100	2.116	2.096	2.058	2.100	2.063	2.119	2.061
Al	0.911	0.906	0.887	0.900	0.905	0.892	0.923	0.954	0.898	0.951	0.896	0.949
Fe	0.001	–	–	–	0.001	–	0.000	0.002	0.001	–	0.001	0.004
Mn	–	0.001	–	–	–	–	0.001	–	–	0.001	0.000	–
Mg	0.002	–	–	–	–	0.001	0.003	–	–	0.003	–	–
Na	0.152	0.167	0.135	0.170	0.133	0.117	0.225	0.197	0.229	0.162	0.183	0.170
K	0.006	0.004	0.001	0.001	0.001	0.003	0.001	0.000	0.001	0.001	0.001	0.000
Rb	0.003	0.004	0.002	0.002	0.004	0.004	0.001	0.002	0.002	0.001	0.001	0.002
Cs	0.637	0.672	0.675	0.697	0.749	0.731	0.525	0.703	0.584	0.724	0.566	0.735
Ca	0.001	0.000	0.000	0.000	–	0.000	0.002	0.001	–	–	0.000	–
P	0.001	0.001	0.001	–	–	0.001	0.017	–	0.018	–	0.017	–
Si/Al	2.32	2.33	2.40	2.34	2.32	2.37	2.27	2.16	2.34	2.17	2.37	2.17
Pol	79.57	79.39	82.96	80.25	84.66	85.42	69.42	77.99	71.60	81.36	75.32	80.99
CRK	80.62	80.26	83.42	80.34	84.95	86.22	69.56	78.13	71.95	81.51	75.61	81.23

Structural formulae are calculated based on 6 atoms of oxygen per formula unit (*apfu*). –: below detection limits. For heterogeneous pollucite of yc09, D and B correspond darker and lighter parts on BSE images, respectively. Results of electron-microprobe analyses.

topaz–lepidolite granite described below shows systematic compositional features of such a type of cesian mica. As shown below, the Cs-dominant lepidolite found in the Yichun granite is in fact the Cs-dominant analogue of polyolithionite, which we will shorten as “Cs-dominant Pln” hereafter.

#### Composition of the lepidolite-series minerals

In the Yichun topaz–lepidolite granite, lepidolite is one of the major rock-forming minerals. It usually occurs as fine tabular crystals in the groundmass, and corresponds chemically to the polyolithionite–trilithionite solid solution, and to the Li-bearing muscovite end-member (Belkasmı *et al.* 1992). The composition of the lepidolite, like the feldspar, differs depending on the petrographic facies. In the K-feldspar-rich facies of the granite, the mica corresponds to (Fe,Mn)-bearing lepidolite (Zk15: FeO = 1.08 wt%, Mn = 1.63 wt%, Table 2). Purer lepidolite is observed in the albite-rich facies: Fe and Mn are generally less than 0.30 wt% FeO and 1.00% MnO, respectively. Noteworthy is the occurrence of zinnwaldite, instead of lepidolite, at the near-surface sample of the upper part (on average 6.64 wt% FeO and 2.06 wt% MnO in sample Zk3).

Rb and Cs are two components of the lepidolite structure. Concentrations of Rb are virtually constant, oscillating around 1 wt% (Table 2). Most of the lepidolite flakes contain generally less than 1 wt% Cs<sub>2</sub>O (Table 2). In the albite-rich facies, however, the lepidolite is characterized by enrichment in Cs. Our detailed study has revealed a Cs-bearing to Cs-dominant Pln.

#### Zonation of Cs-rich lepidolite-series minerals

Two types of occurrence of the cesian-lepidolite-series minerals are described below, one consists of inclusions of Cs-rich polyolithionite within rock-forming minerals, the other represents a Cs-rich rim around the primary lepidolite-series minerals.

In the albite-rich facies of the granite (Zk5, 6, 7, YC08), a Cs-rich lepidolite-series mineral is found included in various rock-forming minerals, mainly K-feldspar and albite. In the K-feldspar phenocrysts with the “snowball” texture, lepidolite laths of about 10 μm long and a few μm wide contribute to this texture (Fig. 4). It must be noted that the lepidolite is restricted to the host K-feldspar phenocrysts, and is never found in their albite inclusions. In addition, the lepidolite displays zoning, with a darker core and a thin lighter rim in

TABLE 2. AVERAGE COMPOSITION OF LEPIDOLITE IN SELECTED SAMPLES FROM THE YICHUN TOPAZ–LEPIDOLITE GRANITE, SOUTHERN CHINA

<i>n</i>	Zk15 15	Zk13 5	Zk9 10	Zk8 4	Zk7 6	Zk6 5	Zk4 7	Zk3 5
SiO <sub>2</sub> wt%	49.58(1.23)	50.19(1.60)	50.76(0.89)	50.67(0.79)	50.94(0.96)	51.11(0.67)	49.25(2.40)	47.57(1.74)
Al <sub>2</sub> O <sub>3</sub>	23.59(0.96)	23.45(0.47)	24.05(0.42)	23.68(0.99)	23.80(0.85)	23.81(0.98)	23.02(1.23)	23.82(1.92)
FeO	1.08(0.50)	0.54(0.12)	0.28(0.09)	0.17(0.11)	0.11(0.08)	0.12(0.05)	0.21(0.12)	6.64(0.38)
MnO	1.63(0.43)	1.23(0.22)	0.77(0.33)	0.67(0.27)	0.44(0.14)	0.47(0.27)	0.43(0.15)	2.06(0.20)
MgO	0.01(0.02)	0.00(0.00)	0.01(0.02)	0.01(0.02)	0.01(0.01)	0.01(0.02)	0.01(0.00)	0.01(0.02)
Li <sub>2</sub> O	4.68(0.35)	4.85(0.46)	5.02(0.26)	4.99(0.23)	5.07(0.28)	5.12(0.19)	4.58(0.69)	4.10(0.50)
Na <sub>2</sub> O	0.20(0.05)	0.17(0.04)	0.18(0.04)	0.16(0.05)	0.12(0.04)	0.11(0.05)	0.16(0.06)	0.14(0.04)
K <sub>2</sub> O	10.51(0.28)	10.51(0.13)	10.54(0.29)	10.41(0.66)	10.57(0.21)	10.45(0.33)	10.11(0.85)	10.78(0.18)
Rb <sub>2</sub> O	1.07(0.13)	1.05(0.11)	1.01(0.14)	1.01(0.12)	1.17(0.20)	0.97(0.19)	1.17(0.18)	0.79(0.14)
Cs <sub>2</sub> O	0.10(0.07)	0.06(0.04)	0.08(0.04)	0.35(0.54)	0.38(0.25)	0.33(0.35)	0.32(0.34)	0.05(0.05)
CaO	0.01(0.01)	0.01(0.01)	0.01(0.01)	0.01(0.02)	0.00(0.00)	0.01(0.02)	0.01(0.01)	0.01(0.01)
F	7.77(0.77)	7.68(0.47)	8.20(0.69)	8.02(0.59)	8.52(0.24)	8.31(0.79)	7.83(0.58)	5.53(0.69)
F=O	3.26	3.23	3.44	3.37	3.58	3.49	3.29	2.32
Total	96.97	96.51	97.47	96.78	97.55	97.33	93.81	99.18
Si <i>apfu</i>	3.39	3.43	3.44	3.45	3.46	3.46	3.47	3.16
<sup>IV</sup> Al	0.61	0.57	0.56	0.55	0.54	0.54	0.53	0.84
<sup>VI</sup> Al	1.29	1.32	1.35	1.36	1.36	1.36	1.38	1.02
Fe	0.06	0.03	0.02	0.01	0.01	0.01	0.01	0.37
Mn	0.09	0.07	0.04	0.04	0.03	0.03	0.03	0.12
Mg	0.00	0.00	0.00	0.00	0.00	0.00	0.00	0.00
Li	1.29	1.33	1.36	1.37	1.38	1.39	1.29	1.09
Σ	2.74	2.76	2.78	2.77	2.78	2.80	2.71	2.60
Na	0.03	0.02	0.02	0.02	0.02	0.01	0.02	0.02
K	0.92	0.92	0.91	0.91	0.92	0.90	0.91	0.91
Rb	0.05	0.05	0.04	0.04	0.05	0.04	0.05	0.03
Cs	0.00	0.00	0.00	0.01	0.01	0.01	0.01	0.00
Ca	0.00	0.00	0.00	0.00	0.00	0.00	0.00	0.00
Σ	0.99	0.99	0.98	0.98	0.99	0.97	0.99	0.97
F	1.68	1.66	1.75	1.73	1.83	1.78	1.75	1.16
OH	0.32	0.34	0.25	0.27	0.17	0.22	0.25	0.84

Structural formulae are calculated on the basis of 11 atoms of oxygen per formula unit (*apfu*). The amount of Li<sub>2</sub>O is estimated using the empirical equation of Tindle & Webb (1990). OH = 2 – F. Average results of *n* electron-microprobe analyses.

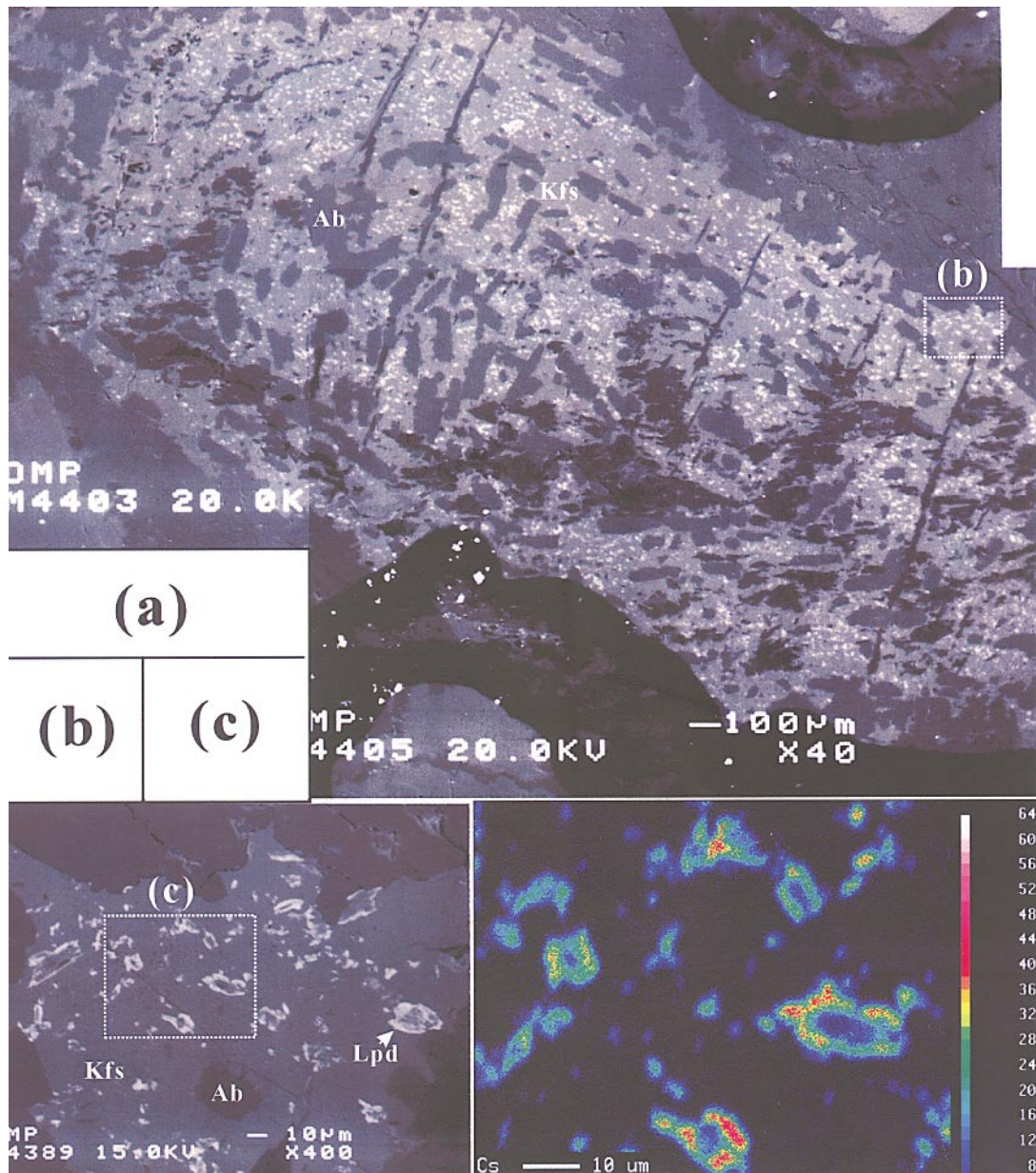


FIG. 4. Cs-rich lepidolite inclusions in a K-feldspar phenocryst with a “snowball” texture. (a) Back-scattered electron image. (b) Enlargement of the selected area in Figure 4a reveals a zonation, with Cs enrichment at the rim. (c) Distribution map of Cs of the selected part in Figure 4b. Same symbols as in Figure 2.

back-scattered electron images (Fig. 4b). A similar zonal texture of lepidolite has already been described in the pegmatite of Moldanubicum (Teerststra *et al.* 1995). Both elemental mapping and spot analyses reveal a nor-

mally Cs-bearing core and a highly Cs-enriched rim (Fig. 4c, Table 3). The sharp core–rim boundary is caused by distinctive Cs contents between the two parts. The cores commonly contain less than 4 wt% Cs<sub>2</sub>O,

whereas the greater amounts, up to 25 wt% Cs<sub>2</sub>O, typify the rim.

Outside the K-feldspar phenocrysts, the albite groundmass can also contain inclusions of lepidolite, but less commonly. Chemically, this type of lepidolite displays the same zonation as that described above (Fig. 5). The core is slightly enriched in Cs (Cs<sub>2</sub>O < 2 wt%), whereas the rim may contain up to 22 wt% Cs<sub>2</sub>O.

In addition, we note the presence of a Cs-rich rim on lepidolite flakes in the groundmass in the middle to upper parts of the albite-rich facies, particularly well displayed in samples Zk6, Zk7 and Yc08. The Cs-rich zone normally replaces rock-forming lepidolite flakes (Figs. 6a). It may also occur as fine subparallel laths penetrating along cleavages of the host lepidolite (Fig. 6b). The Cs-rich rims are several micrometers wide. The primary lepidolite contains generally <1 wt% Cs<sub>2</sub>O, whereas Cs<sub>2</sub>O concentrations at its rim are generally >17 wt%, and up to 25.81 wt% Cs<sub>2</sub>O (Table 4). Similarly, some Li-bearing muscovite was also replaced by the Cs-rich end-member composition at its rim (Table 4).

#### Raman spectra of the Cs-dominant Pln

It is impossible to analyze the Cs-dominant Pln with X-ray diffraction owing to the difficulty of mineral separation. For this reason, we chose Raman spectroscopy to make a comparison of the Cs-dominant Pln with a Cs-bearing lepidolite-series mineral.

Representative Raman scattering spectra recorded on both the Cs-rich rim (Cs-dominant Pln, 16.8 wt% Cs<sub>2</sub>O)

and Cs-bearing lepidolite (0.6 wt% Cs<sub>2</sub>O) of an albite-hosted zoned inclusion of lepidolite are presented in Figure 7. On the basis of previous results of McKeown *et al.* (1999a, b) and Wang *et al.* (2002), Raman peaks may be assigned. The peak at about 1150 cm<sup>-1</sup> is attributed to the stretching mode of the Si–O<sub>nb</sub> bond (O<sub>nb</sub>: non-bridging oxygen) in SiO<sub>4</sub> tetrahedra. The typical peak for phyllosilicate minerals at ~700 cm<sup>-1</sup> is well displayed for both the Cs-dominant Pln and Cs-bearing lepidolite, corresponding to both Si–O stretching and O–Si–O bending deformations. This is the result of the deviation of mica compositions toward a “tetrasilicic” trioctahedral mica (Wang *et al.* 2002). The Raman peaks in the <600 cm<sup>-1</sup> region arise from a complex set of translational motions of cations in octahedral sites and in interlayer sites relative to the SiO<sub>4</sub> groups in the layers of tetrahedra, the oxygen atoms, and the OH groups (including their transitional and librational motions).

The Raman spectra of the two parts of the lepidolite, distinctive in Cs content, are very similar in their peak positions, and are furthermore comparable with the Raman spectrum published by Wang *et al.* (2002). Therefore, we suggest that a Cs-bearing, even a Cs-dominant, member of the lepidolite series is structurally the same as a mineral of the lepidolite series.

#### Crystal chemistry of Cs-rich lepidolite-series minerals

As in the solid-solution series muscovite – nanpingite or phlogopite – cesian phlogopite, a good correlation exists between K and Cs in the series between lepidol-

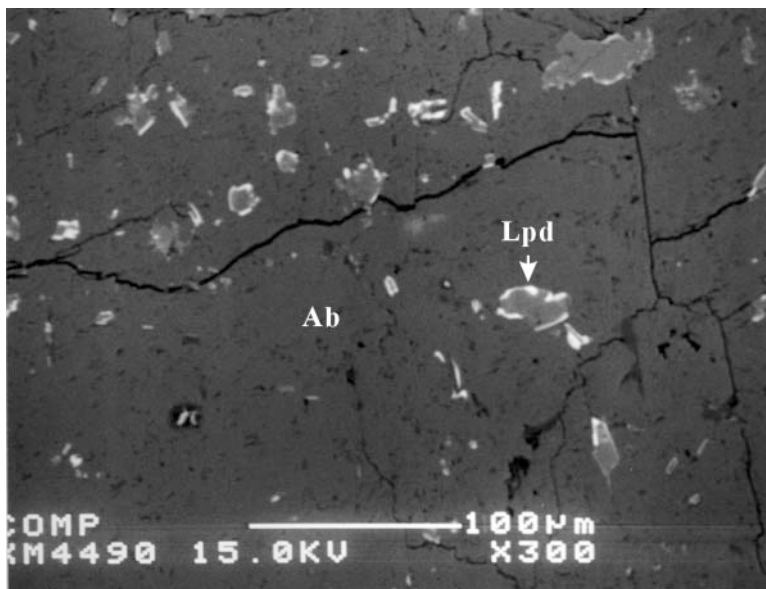


FIG. 5. Back-scattered electron image of Cs-bearing zoned lepidolite in an albite crystal. Same symbols as in Figure 2.

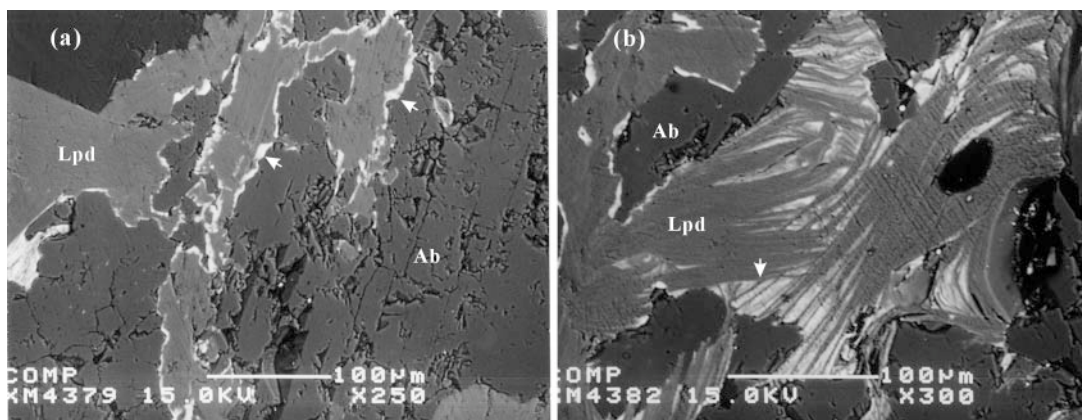


FIG. 6. Back-scattered electron images of Cs-rich lepidolite. (a) Cs-rich zone (indicated by arrow) replacing the primary lepidolite at the rim. (b) Cs-rich zones (indicated by arrow) penetrating along the cleavage of the primary lepidolite. Same symbols as in Figure 2.

TABLE 3. REPRESENTATIVE COMPOSITIONS OF ZONED LEPIDOLITE INCLUSIONS IN FELDSPARS FROM THE YICHUN TOPAZ–LEPIDOLITE GRANITE, SOUTHERN CHINA

	Inclusions in K-feldspar phenocrysts						Inclusions in albite					
	21 Core	22 Rim	34 Core	35 Rim	36 Core	37 Rim	1 Core	2 Rim	6 Core	5 Rim	30 Core	29 Rim
SiO <sub>2</sub> wt%	52.23	47.21	52.78	48.53	55.07	49.32	52.11	47.76	48.38	46.75	52.64	47.75
Al <sub>2</sub> O <sub>3</sub>	19.81	17.41	20.05	16.04	16.43	15.11	23.02	16.85	28.79	16.86	22.59	18.14
FeO	—	—	—	0.05	0.09	—	0.07	0.10	—	—	0.04	—
MnO	—	0.14	0.09	0.15	0.01	—	0.12	—	—	0.05	—	0.09
MgO	—	—	0.03	—	—	0.01	—	—	—	0.01	—	—
Li <sub>2</sub> O	5.44	4.00	5.60	4.38	6.25	4.60	5.40	4.15	4.33	3.87	5.56	4.15
Na <sub>2</sub> O	0.02	—	0.03	0.03	0.00	0.03	0.10	0.43	0.05	0.10	0.04	0.13
K <sub>2</sub> O	8.86	2.26	9.98	2.45	9.53	2.07	10.77	1.10	10.74	0.93	11.07	2.59
Rb <sub>2</sub> O	0.88	0.44	0.76	0.36	0.80	0.49	0.77	0.49	0.63	0.24	0.70	0.39
Cs <sub>2</sub> O	4.96	22.25	3.25	21.99	2.71	21.05	0.67	21.82	1.29	23.12	0.92	19.98
CaO	0.05	—	—	0.04	0.01	0.04	0.00	0.02	0.03	0.06	0.01	0.02
F	8.76	5.88	9.67	6.32	9.08	6.97	6.73	7.30	4.58	7.34	6.57	7.34
F=O	3.68	2.47	4.06	2.65	3.81	2.93	2.83	3.07	1.92	3.08	2.76	3.08
Total	97.33	97.12	98.18	97.69	96.17	96.76	96.93	96.95	96.90	96.25	97.38	97.50
Si <i>apfu</i>	3.647	3.718	3.632	3.786	3.813	3.857	3.508	3.761	3.248	3.751	3.531	3.695
<sup>IV</sup> Al	0.353	0.282	0.368	0.214	0.187	0.143	0.492	0.239	0.752	0.249	0.469	0.305
<sup>VI</sup> Al	1.277	1.334	1.258	1.261	1.154	1.250	1.334	1.325	1.526	1.346	1.316	1.349
Fe	0.000	0.000	0.000	0.003	0.005	0.000	0.004	0.006	0.000	0.000	0.002	0.000
Mn	0.000	0.009	0.005	0.010	0.001	0.000	0.007	0.000	0.000	0.004	0.000	0.006
Mg	0.000	0.000	0.003	0.000	0.000	0.001	0.000	0.000	0.000	0.001	0.000	0.000
Li	1.527	1.266	1.549	1.373	1.742	1.447	1.463	1.316	1.170	1.248	1.499	1.292
Σ	2.804	2.609	2.814	2.647	2.901	2.699	2.808	2.647	2.696	2.597	2.817	2.646
Na	0.003	0.000	0.004	0.004	0.001	0.004	0.013	0.066	0.006	0.016	0.005	0.020
K	0.789	0.227	0.876	0.244	0.842	0.206	0.925	0.110	0.920	0.095	0.947	0.256
Rb	0.039	0.022	0.033	0.018	0.036	0.024	0.033	0.025	0.027	0.012	0.030	0.019
Cs	0.148	0.747	0.095	0.731	0.080	0.701	0.019	0.732	0.037	0.791	0.026	0.659
Ca	0.004	0.000	0.000	0.003	0.001	0.004	0.000	0.002	0.002	0.005	0.000	0.001
Σ	0.983	0.996	1.009	1.001	0.959	0.940	0.991	0.935	0.993	0.919	1.009	0.955
F	1.935	1.463	2.104	1.558	1.987	1.725	1.433	1.819	0.972	1.863	1.394	1.795
OH	0.065	0.437	—	0.442	0.013	0.275	0.467	0.181	0.028	0.137	0.606	0.205

Structural formulae are calculated on the basis of 11 atoms of oxygen per formula unit (*apfu*). The amount of Li<sub>2</sub>O is estimated using the empirical equation of Tindle & Webb (1990). —: below detection limits. OH = 2 – F. Results of electron-microprobe analyses.

TABLE 4. REPRESENTATIVE COMPOSITIONS OF Cs-RICH RIM REPLACING PRIMARY LEPIDOLITE AND MUSCOVITE IN THE YICHUN TOPAZ-LEPIDOLITE GRANITE, SOUTHERN CHINA

	Zk7					Zk6				Zk8		
	11	12	13	14	30	31	8	9	7	8*	08-6	7*
SiO <sub>2</sub> wt%	49.39	47.51	46.70	50.58	46.96	46.48	47.52	51.07	49.10	45.07	48.70	46.53
Al <sub>2</sub> O <sub>3</sub>	24.70	17.36	16.45	23.42	16.20	16.52	16.39	23.96	17.73	33.63	16.32	34.62
FeO	0.16	–	0.07	0.10	–	–	0.00	0.13	–	–	0.43	–
MnO	0.41	0.18	0.17	0.39	0.18	0.15	0.16	0.63	–	0.01	0.56	0.07
MgO	–	0.04	0.01	–	–	–	–	–	0.01	–	–	–
Li <sub>2</sub> O	4.62	4.08	3.85	4.97	3.92	3.79	4.09	5.10	4.54	3.38	4.42	3.80
Na <sub>2</sub> O	0.15	0.42	0.24	0.13	0.02	0.10	0.11	0.08	1.15	0.16	0.01	0.06
K <sub>2</sub> O	10.39	1.28	1.58	10.35	0.64	0.69	1.22	10.13	1.54	11.15	2.86	11.12
Rb <sub>2</sub> O	1.27	0.31	0.40	1.32	0.27	0.17	0.43	1.04	0.46	0.33	0.63	0.46
Cs <sub>2</sub> O	0.41	22.48	22.83	0.50	25.81	25.50	23.76	0.15	19.79	0.34	20.67	0.20
CaO	–	0.05	0.05	–	0.01	0.02	0.02	0.00	0.06	–	0.07	–
F	8.50	6.56	6.78	8.65	5.97	6.15	6.61	8.60	6.59	1.05	7.36	1.41
F=O	3.57	2.76	2.85	3.63	2.51	2.58	2.78	3.61	2.77	0.44	3.09	0.59
Total	96.43	97.51	96.28	96.48	97.47	96.99	97.53	97.28	98.20	94.68	98.94	97.68
Si <i>apfu</i>	3.403	3.725	3.754	3.472	3.781	3.758	3.773	3.457	3.715	3.026	3.749	3.021
<sup>IV</sup> Al	0.597	0.275	0.246	0.528	0.219	0.242	0.227	0.543	0.285	0.974	0.251	0.979
<sup>VI</sup> Al	1.409	1.329	1.312	1.366	1.318	1.332	1.308	1.369	1.296	1.686	1.230	1.671
Fe	0.009	0.000	0.005	0.006	0.000	0.000	0.000	0.008	0.000	0.000	0.028	0.000
Mn	0.024	0.012	0.011	0.023	0.012	0.010	0.011	0.036	0.000	0.001	0.037	0.004
Mg	0.000	0.005	0.002	0.000	0.000	0.000	0.000	0.000	0.001	0.000	0.000	0.000
Li	1.281	1.287	1.245	1.371	1.271	1.232	1.305	1.390	1.382	0.914	1.370	0.993
Σ	2.723	2.633	2.575	2.766	2.601	2.575	2.623	2.803	2.678	2.601	2.664	2.668
Na	0.020	0.064	0.037	0.017	0.003	0.015	0.017	0.011	0.168	0.021	0.001	0.008
K	0.913	0.128	0.162	0.906	0.066	0.071	0.123	0.875	0.148	0.955	0.281	0.921
Rb	0.056	0.016	0.021	0.058	0.014	0.009	0.022	0.045	0.022	0.014	0.031	0.019
Cs	0.012	0.751	0.782	0.015	0.886	0.879	0.804	0.004	0.638	0.010	0.678	0.006
Ca	0.000	0.004	0.004	0.000	0.001	0.002	0.002	0.000	0.004	0.000	0.006	0.000
Σ	1.001	0.963	1.007	0.996	0.969	0.976	0.968	0.936	0.981	1.000	0.997	0.953
F	1.853	1.627	1.723	1.878	1.519	1.573	1.660	1.842	1.577	0.223	1.791	0.290
OH	0.147	0.373	0.277	0.122	0.481	0.427	0.340	0.158	0.423	0.777	0.209	0.710

Structural formulae are calculated on the basis of 11 atoms of oxygen per formula unit (*apfu*). The amount of Li<sub>2</sub>O is estimated using the empirical equation of Tindle & Webb (1990). –: below detection limits. OH = 2 – F. Results of electron-microprobe analyses. \*: muscovite.

ite and Cs-rich lepidolite (Fig. 8). This relationship indicates a reasonable K ↔ Cs substitution for the Cs-rich lepidolite, suggesting its structural formula as (K, Cs)(Li,Al)<sub>3</sub>[(Al,Si)<sub>4</sub>O<sub>10</sub>](F,OH)<sub>2</sub>. It must be noted that the Cs may exceed 0.5 atoms per formula unit (*apfu*) in our material, and may reach values as high as 0.89 *apfu*. The lepidolite-series member thus varies in terms of Cs-for-K substitution. Figure 9 shows the relative proportions of the major interlayer-site cations (Cs, K and Rb) in the lepidolite from the Yichun granite. The material studied is very close to the K – Cs join, in contrast to the Rb- and Cs-rich polyolithionite from the Red Cross Lake granitic pegmatite (Černý *et al.* 2003). Values of Rb/K are rather low in the lepidolite, possibly because of overall low concentrations of Rb in the pegmatite-forming melt at Altai. No Rb-bearing minerals have been found in the Altai granitic pegmatite.

According to the nomenclature of the micas (Rieder *et al.* 1998), *lepidolite* refers to a series of micas on, or close to, the join trilithionite K(Li<sub>1.5</sub>Al<sub>1.5</sub>)[AlSi<sub>3</sub>O<sub>10</sub>](F,OH)<sub>2</sub> – polyolithionite K(Li<sub>2</sub>Al)[Si<sub>4</sub>O<sub>10</sub>](F,OH)<sub>2</sub>. In the case where Cs is dominant at the interlayer site in the structure, analogues of trilithionite and polyolithionite, Cs(Li<sub>1.5</sub>Al<sub>1.5</sub>)[AlSi<sub>3</sub>O<sub>10</sub>](F,OH)<sub>2</sub> and Cs(Li<sub>2</sub>Al)[Si<sub>4</sub>O<sub>10</sub>](F,OH)<sub>2</sub>, can be expected. A diagram of Cs/(K + Cs) versus <sup>IV</sup>Al is proposed to distinguish the end-members of the lepidolite series and their Cs analogues (Fig. 10). The data from the present study were plotted in this diagram. The estimated <sup>IV</sup>Al of the material studied ranges from 0.09 to 0.94 *apfu*, mostly in the range of 0.09 and 0.40 *apfu* for the Cs-rich zoned lepidolite, which is thus dominated by the polyolithionite end-member. In terms of the ratio Cs/(K + Cs), the data-points were divided into three groups. The Cs/(K + Cs)

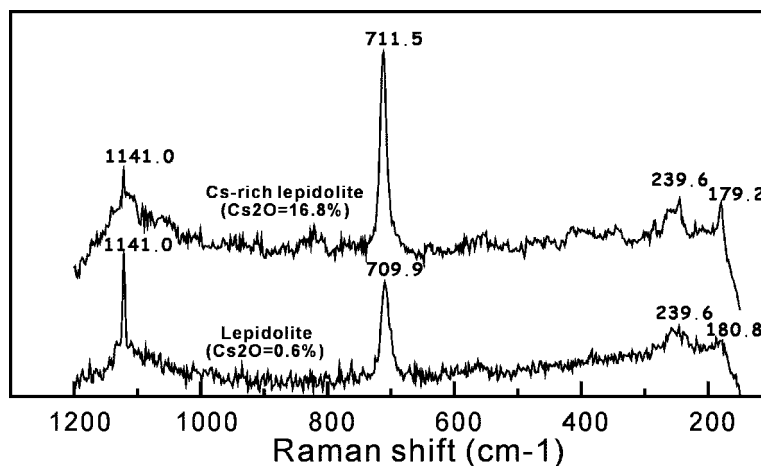


FIG. 7. Micro-Raman spectra of lepidolite and Cs-rich lepidolite in the spectral region 100 to 1200  $\text{cm}^{-1}$ .

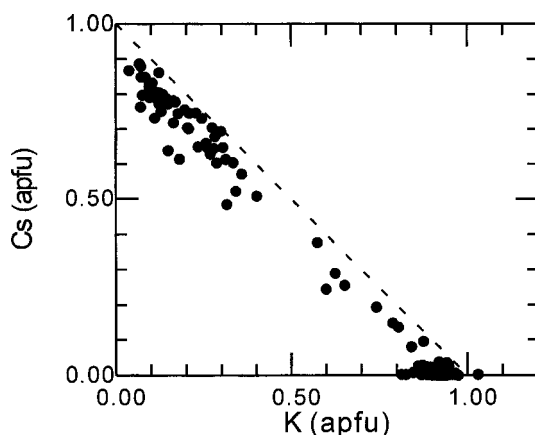


FIG. 8. Plots of concentrations of K versus Cs in the lepidolite, with concentrations expressed in atoms per formula unit, apfu.

value of the lepidolite flakes in the groundmass is  $<0.1$ , whereas the zoned lepidolite is more enriched in Cs. The core of the zoned lepidolite has a  $\text{Cs}/(\text{K} + \text{Cs})$  value of 0.1 to 0.4, in contrast to the rim, with a ratio generally exceeding 0.5, even up to 0.96. Therefore, the zoned lepidolite rims correspond to a Cs-dominant analogue of polyolithionite. In Figure 9b, one sees that even though there are micas of trilithionite composition, there is virtually no Cs enrichment in these minerals. It is only the samples of polyolithionite that exhibit Cs enrichment. The data of Černý *et al.* (2003) and those of the Altai granitic pegmatite (Wang *et al.*, in prep.) also reveal that

Cs enrichment is found in polyolithionite. That said, there is no evidence presented that would support the designation of a Cs-dominant analogue of trilithionite. However, more work needs to be done to understand the existence of Cs in the structure of trilithionite.

#### DISCUSSION

The Yichun topaz–lepidolite granite is highly evolved, with economic concentrations of disseminated rare metals such as Li, Ta, Nb and Be. It also shows an enrichment in rare alkalis. Like other rare-metal accessory minerals (Huang *et al.* 2002), Cs minerals are very sensitive to the physicochemical conditions of their environment of crystallization in the leucogranitic magma. According to their distribution and compositional features, Cs minerals seem to have formed at the late-magmatic stage and at the transition from magmatic to hydrothermal conditions.

#### *Crystallization of Cs minerals in the Yichun topaz–lepidolite granite*

The enrichment of the melt in Cs, and in volatile components such as F, B and P, promotes a decrease in the solidus temperature of the granitic melt (London *et al.* 1998). However, Cs is an incompatible element in major rock-forming minerals such as quartz ( $K^{\text{quartz/melt}} < 0.01$ , Audétat & Pettker 2003), alkali feldspar ( $K^{\text{alkali feldspar/melt}} < 0.1$ , Icenhower & London 1996, Morgan & London 2003), as well as plagioclase ( $K^{\text{plagioclase/melt}} < 0.04$ , Audétat & Pettker 2003). Therefore, Cs may be progressively enriched in the melt with advancing crystallization (Veksler & Thomas 2002, Audétat & Pettker 2003). Muscovite – melt partition coefficients for Cs

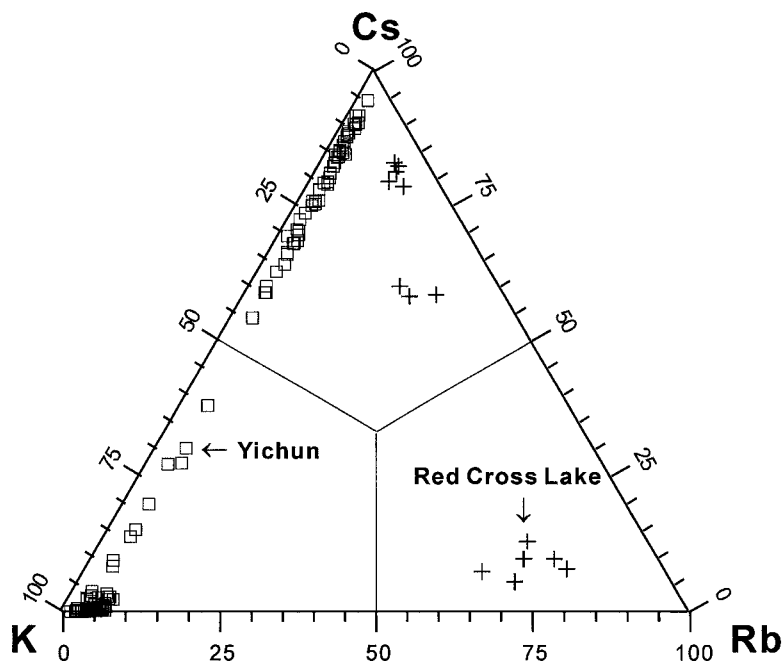


FIG. 9. Plots of compositions of Yichun lepidolite (open square) in terms of Cs, K, and Rb. Rb- and Cs-dominant polyolithionite (cross) from the Red Cross Lake granitic pegmatites (Cerný *et al.* 2003) are plotted for comparison.

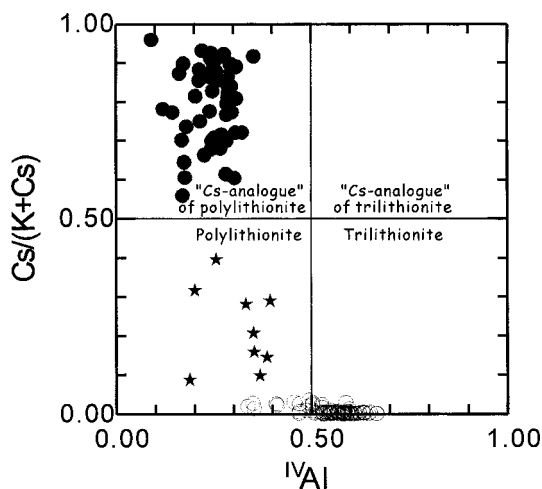


FIG. 10. Plots of compositions of lepidolite from the Yichun topaz-lepidolite granite in terms of  $IVAl$  (*apfu*) versus  $Cs/(K+Cs)$ . Open circles: lepidolite flakes, solid circles: rim of zoned lepidolite, stars: core of zoned lepidolite.

were determined by various methods, but the values obtained match very closely. Experimentally determined partition coefficients are in the range of 0.16 to 0.23 (Icenhower & London 1996). Similarly calculated muscovite – rock values in the Richemont rhyolite (France) varies between 0.2 and 0.4 (Raimbault & Burnol 1998). Although the Cs partition coefficients obtained between muscovite and melt are lower than unity, the fact that cesian phlogopite, cesian biotite, and even nannigite exist in some pegmatitic environments indicates that micas, including muscovite, are certainly good hosts for Cs. In the Yichun topaz-lepidolite granite, cesium becomes more enriched in residual melt with fractional crystallization of the leucogranitic magma, and attains the greatest concentrations at the upper part of the albite-rich facies of the granite (Fig. 1). At this late-magmatic stage, primary minerals of Cs (pollucite or Cs-rich lepidolite) crystallize as inclusions within rock-forming minerals (quartz, K-feldspar or albite), particularly as small inclusions of zoned Cs-rich lepidolite within K-feldspar or albite. It is very interesting to note that in their run products at 450°C, 0.1 GPa, Veksler & Thomas (2002) identified a Cs-bearing aluminosilicate (9.27 wt%  $Cs_2O$ ) by electron-microprobe analysis [calculated structural formula:  $(Na,K,Rb,Cs)_3(Si,Al,P)_{14}O_{32}(OH)_6$ ], which looks like a Cs-bearing near-solidus phase.

Pollucite is intergrown with K-feldspar, spodumene, or petalite (*e.g.*, Tanco, Manitoba, Černý & Simpson 1978, Bikita, Zimbabwe, Teertstra & Černý 1997) and also associated with lepidolite, elbaite, and montebrazite, suggesting that the formation of pollucite in granitic pegmatites occurs at the transition from magmatic to hydrothermal conditions (London *et al.* 1998). In our case, pollucite may also crystallize around rock-forming minerals, in particular as large crystals filling interstices among tabular crystals of albite. Such pollucite appears to have formed prior to the complete crystallization of the silicate melt. As indicated by London *et al.* (1998), the formation of this type of pollucite in the Yichun topaz–lepidolite granite seems to occur during the evolution of the magmatic to hydrothermal stage.

Fluid–melt partition coefficients for Cs published by Webster *et al.* (1989) are variable, but they can be expected to increase as temperature decreases at 0.5 kbar. In fact, the Cs contents in magmatic fluids should increase with progressive crystallization of granitic magma (Audétat & Pettker 2003). The fact that pollucite and nanpingite-like mica occur as pocket phases in the lithium pegmatite of the O'Grady batholith (Ercit *et al.* 2003) indicates also that Cs enrichment in fluid is likely. In the case of the Yichun topaz–lepidolite granite, Cs-bearing fluids may have exsolved during the evolution of the leucogranitic magma. This type of fluid further replaced the early-formed lepidolite along the marginal part or cleavages (Figs. 6a, b), thus leading to formation of Cs-rich lepidolite in the upper middle part of the granite.

#### *Comparison with crystallization process of rare-element minerals*

Huang *et al.* (2002) carried out a systematic study on rare-element accessory minerals in the Yichun topaz–lepidolite granite. Like the Cs-bearing minerals, rare-element-bearing minerals display important variations in composition as a function of depth. Columbite and zircon are present throughout the granite, and display progressive increases in Ta/(Nb + Ta) and Hf content, respectively, from the lower part to the middle part of the drill hole, suggestive of magmatic differentiation at the beginning of crystallization after the intrusion of the magma at shallower level. However, unlike columbite and zircon, pollucite as well as Cs-rich lepidolite are never observed in the lower part of the granite, and appear only in the middle part of the granite. Experimental results (London *et al.* 1998) reveal that near the solidus of pegmatite-forming melt (at ~640°C), the Cs content of the melt must reach ~5 wt% Cs<sub>2</sub>O to be saturated in pollucite solid-solution. The high Cs content needed to stabilize the pollucite in the granitic melt may explain the absence of this phase at the early stage of crystallization in the Yichun topaz–lepidolite granite.

#### ACKNOWLEDGEMENTS

Financial support for this work was provided by the Natural Science Foundation of China (40025209, 40221301 and 40302010) and by the Chinese Ministry of Education (2000028431). Reviews by W.B. Simmons, Jr. and A.U. Falster, and the editorial efforts of R.F. Martin, significantly improved the content and presentation of this paper. RCW thanks F. Fontan for many fruitful discussions both in Nanjing and in Toulouse.

#### REFERENCES

- ARMSTRONG, J.T. (1989): CITZAF: combined ZAF and rho(Z) electron beam correction programs. California Institute of Technology, Pasadena, California.
- AUDÉTAT, A. & PETTKER, T. (2003): The magmatic-hydrothermal evolution of two barren granites: a melt and fluid inclusion study of the Rito del Medio and Cañada Pinabete plutons in northern New Mexico (USA). *Geochim. Cosmochim. Acta* **67**, 97–121.
- BELKASMI, M., CUNNEY, M. & POLLARD, P.J. (1992): Micas and niobotantalates as indicators of petrogenetic evolution of rare-metal granites. The example of Yashan granitic complex (SE China). *Symp. "Lepidolite 2000" (Brno, Czechoslovakia)*, 13–14 (abstr.).
- BEGER, R.M. (1969): The crystal structure and chemical composition of pollucite. *Z. Kristallogr.* **129**, 280–302.
- ČERNÝ, P. (1974): The present status of the analcime–pollucite series. *Can. Mineral.* **12**, 334–341.
- \_\_\_\_\_, CHAPMAN, R., TEERTSTRA, D.K. & NOVÁK, M. (2003): Rubidium- and cesium-dominant micas in granitic pegmatites. *Am. Mineral.* **88**, 1832–1835.
- \_\_\_\_\_ & SIMPSON, F.M. (1978): The Tanco pegmatite at Bernic Lake, Manitoba. X. Pollucite. *Can. Mineral.* **16**, 325–333.
- ERCIT, T.S., GROAT, L.A. & GAULT, R.A. (2003): Granitic pegmatites of the O'Grady batholith, N.W.T., Canada: a case study of the evolution of the elbaite subtype of rare-element granitic pegmatite. *Can. Mineral.* **41**, 117–137.
- GINSBURG, A.I., LUGOVSKOI, G.P. & RYABENKO, V.E. (1972): Cesian mica – a new type of mineralization. *Geol. Mineral. Res.* **8**, 1–7 (in Russ.).
- HAWTHORNE, F.C., TEERTSTRA, D.K. & ČERNÝ, P. (1999): Crystal-structure refinement of a rubidian cesian phlogopite. *Am. Mineral.* **84**, 778–781.
- HUANG, XIAO LONG, WANG, RU CHENG, CHEN, XIAO MING, HU, HUAN & LIU, CHANG SHI (2002): Vertical variations in the mineralogy of the Yichun topaz–lepidolite granite, Jiangxi Province, southern China. *Can. Mineral.* **40**, 1047–1068.

- ICENHOWER, J. & LONDON, D. (1996): Experimental partitioning of Rb, Cs, Sr, and Ba between alkali feldspar and peraluminous melt. *Am. Mineral.* **81**, 719-734.
- LONDON, D., MORGAN, G.B., VI & ICENHOWER, J. (1998): Stability and solubility of pollucite in granitic system at 200 MPa H<sub>2</sub>O. *Can. Mineral.* **36**, 497-510.
- MCDONOUGH, W.F., SUN, S.S., RINGWOOD, A.E., JAGOUTZ, E. & HOFMANN, A.W. (1992): Potassium, rubidium and cesium in the Earth and Moon and the evolution of the mantle of the Earth. *Geochim. Cosmochim. Acta* **56**, 1001-1012.
- McKEOWN, D.A., BELL, M.I. & ETZ, E.S. (1999a): Raman spectra and vibrational analysis of the trioctahedral mica phlogopite. *Am. Mineral.* **84**, 970-976.
- \_\_\_\_\_, \_\_\_\_\_ & \_\_\_\_\_ (1999b): Vibrational analysis of the dioctahedral mica: 2M<sub>1</sub> muscovite. *Am. Mineral.* **84**, 1041-1048.
- MORGAN, G.B., VI & LONDON, D. (2003): Trace-element partitioning at conditions far from equilibrium: Ba and Cs distributions between alkali feldspar and undercooled hydrous granitic liquid at 200 MPa. *Contrib. Mineral. Petrol.* **144**, 722-738.
- NI, YUNXIANG & HUGHES, J.M. (1996): The crystal structure of nanpingite-2M<sub>2</sub>, the Cs end-member of muscovite. *Am. Mineral.* **81**, 105-110.
- RAIMBAULT, L. & BURNOL, L. (1998): The Richmond rhyolite dyke, Massif Central, France: a subvolcanic equivalent of rare-metal granites. *Can. Mineral.* **36**, 265-282.
- RIEDER, M. and fourteen others (1998): Nomenclature of the micas. *Can. Mineral.* **36**, 905-912.
- ROSSI, P., AUTRAN, A., AZENCOTT, C., BURNOL, L., CUNEY, M., JOHAN, V., KOSAKEVITCH, A., OHNENSTETTER, D., MONIER, G., PIANTONE, P., RAIMBAULT, L. & VIALLEFOND, L. (1987): Logs pétrographiques et géochimiques du granite de Beauvoir dans le sondage GPF "Echassières I": minéralogie et géochimie comparée. In *Le forage scientifique d'Echassières* (M. Cuney & A. Autran, eds.). *Géologie de la France* **2-3**, 111-135.
- SHANNON, R.D. (1976): Revised effective ionic radii and systematic studies of interatomic distances in halides and chalcogenides. *Acta Crystallogr.* **A32**, 751-767.
- SIMMONS, W.B., PEZZOTTA, F., FALSTER, A.U. & WEBBER, K.L. (2001): Londonite, a new mineral species: the Cs-dominant analogue of rhodizite from the Antandrokomby granitic pegmatite, Madagascar. *Can. Mineral.* **39**, 747-755.
- TEERTSTRA, D.K. & ČERNÝ, P. (1995): First natural occurrences of end-member pollucite: a product of low-temperature reequilibration. *Eur. J. Mineral.* **7**, 1137-1148.
- \_\_\_\_\_, \_\_\_\_\_ & \_\_\_\_\_ (1997): The compositional evolution of pollucite from African granitic pegmatites. *J. Afr. Earth Sci.* **25**, 317-331.
- \_\_\_\_\_, \_\_\_\_\_ & CHAPMAN, R. (1992): Compositional heterogeneity of pollucite from High Grade Dyke, Maskwa Lake, southeastern Manitoba. *Can. Mineral.* **30**, 687-697.
- \_\_\_\_\_, \_\_\_\_\_ & NOVÁK, M. (1995): Compositional and textural evolution of pollucite in pegmatites of the Moldanubicum. *Mineral. Petrol.* **55**, 37-51.
- TINDLE, A.G. & WEBB, P.C. (1990): Estimation of lithium contents in trioctahedral micas using microprobe data: application to micas from granitic rocks. *Eur. J. Mineral.* **2**, 595-610.
- VEKSLER, I.V. & THOMAS, R. (2002): An experimental study of B-, P- and F-rich synthetic granite pegmatite at 0.1 and 0.2 GPa. *Contrib. Mineral. Petrol.* **143**, 673-683.
- WANG, A., FREEMAN, J. & KUEBLER, K.E. (2002): Raman spectroscopic characterization of phyllosilicates. *Lunar Planet. Sci.* **XXXIII**, www.es.lanccs.ac.uk /psrg/abstract/2002.
- WEBSTER, J.D., HOLLOWAY, J.R. & HERVIG, R.L. (1989): Partitioning of lithophile trace elements between H<sub>2</sub>O and H<sub>2</sub>O + CO<sub>2</sub> fluids and topaz rhyolite melt. *Econ. Geol.* **84**, 116-134.
- YANG, YUEQING, NI, YUN XIANG, WANG, LIBEN, WANG, WENYING, ZHANG, YAPING & CHEN, CHENGHU (1988): Nanpingite, a new cesium mineral. *Acta Petrol. Mineral. Sinica* **7**(1), 49-58 (in Chinese with English abstr.).
- YIN, L., POLLARD, P.J., HU, SHOUXI & TAYLOR, R.G. (1995): Geologic and geochemical characteristics of the Yichun Ta-Nb-Li deposit, Jiangxi Province, South China. *Econ. Geol.* **90**, 577-585.

Received August 12, 2003, revised manuscript accepted March 22, 2004.